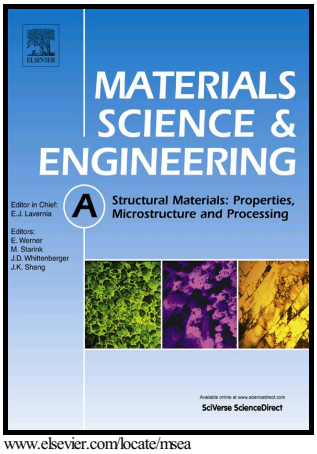

www.elsevier.com/locate/msea

Anelasticity in Cast Mg-Gd Alloys

D. Nagarajan

PII: S0921-5093(17)30408-2
DOI: http://dx.doi.org/10.1016/j.msea.2017.03.094
Reference: MSA34877

To appear in: *Materials Science & Engineering A*

Received date: 7 December 2016
Accepted date: 24 March 2017

Cite this article as: D. Nagarajan, Anelasticity in Cast Mg-Gd Alloys, *Material Science & Engineering A,* http://dx.doi.org/10.1016/j.msea.2017.03.094

Anelasticity in Cast Mg-Gd Alloys

D. Nagarajan*

ARC-Centre of Excellence for Design in Light Metals, Materials Engineering, School of Engineering, The University of Queensland, Brisbane, QLD 4072, Australia

*Current address: Assistant Professor, Department of Metallurgical and Materials Engineering, National Institute of Technology (NIT) Rourkela, Rourkela – 769 008, Odisha State, INDIA. Tel.:+91 661 246 2576; Fax: +91 661 246 2022, E-mail address:nagarajand@nitrkl.ac.in

Abstract

Cyclic loading-unloading tests in tension and compression were carried out on pure Mg and alloys with 0.4, 1.5 and 4.2 at.% Gd, over a range of grain sizes, to quantify the solute and strain dependence of the materials anelasticity in the form of hysteresis loops. For a given grain size, the anelastic effect was more pronounced, i.e., the loops were wider, for pure Mg, and it decreased rapidly with the Gd concentration. The effect was larger for the finer grains in all materials, and in compression for the pure Mg and the 0.4Gd alloy. No difference between tension and compression was observed for the 1.5Gd alloy, whereas the loops were wider in tension than in compression for the 4.2Gd alloy. In comparison with existing studies in Mg-Al and Mg-Zn alloys, for a given solute concentration, Gd was more effective in reducing the magnitude of the effect than either Zn or Al, in that order. The overall behavior is discussed in terms of the hardening effects of short range order of the alloys on $\{10\bar{1}2\}$ and $\{10\bar{1}1\}$ twinning.

Keywords: Anelasticity; Mg-Gd alloys; Mg-Al alloys; Mg-Zn alloys; Short range order; Elastic twinning.

1. Introduction

The activation of twinning at low stress and strains in Mg allows it to play a crucial role, that of indirectly meeting the von-Mises criterion of five independent slip systems, for homogeneous plastic deformation [1-3]. These twins are not fully stable in the deformed state [4] and tend to partly revert, once the applied stress is removed [5] or reversed [6, 7], leading to hysteresis loops during loading and unloading. This type of hysteresis loops have been reported in pure Mg and Mg-Al [5, 6, 8-10], and Mg-Zn [11]. Similar loops have also been observed in Zr [12].

Gharghouri et al. [5, 6] used neutron diffraction to show that the partial reversion of $\{10\bar{1}2\}$ twins upon unloading is the main cause of the loops in pure Mg and Mg-Al. An in-situ study on cast AZ31 alloy [13] also showed that $\{10\bar{1}1\}$ twins form during unloading on grains with the c-axis normal (or nearly so) to the tensile direction, adding to the overall anelastic strain. More recent studies [10, 11] showed that the anelastic strain in Mg-Al first decreased with the Al content (up to 2 at.%) but increased again for the terminal solid solubility (~ 9%Al), whereas in Mg-Zn it decreased monotonically with increasing Zn contents up to the maximum solubility limit (~2.5 at.%). This difference in behavior was ascribed to short range order (SRO) at large Zn concentrations, considering that twinning generally becomes more difficult as ordering sets in [14]. In Mg-Al, Mg-Zn or in pure Mg, the loops were wider in compression than in tension, an effect that accounted for by the polar nature of twinning in conjunction with the tension character of the $\{10\bar{1}2\}$ twins [11, 15]. Under compressive uniaxial stress the volume fraction of twins is larger in compression than under tension, hence the wider loops in the former situation. The increased amount of twinning in

compression leads also to a lower yield strength and in some cases to a plateau in the flow curve, giving rise to a tension-compression asymmetry [10, 16].

More recent work on the Hall-Petch relation of Mg-Gd alloys [17] showed that dilute Mg-Gd alloys reproduced the pattern of behavior just described, i.e., the yield strength was lower in compression and a plateau in the flow curve. At higher concentrations, however, a reversion in the phenomenon occurred: the yield strength was less in tension than in compression. The reversion was explained through the activation of $\{10\bar{1}1\}$ twins. Since these twins are 'compression' in character, (as opposed to 'extension' as $\{10\bar{1}2\}$ twins) the effects upon the yield strength were reversed. The activation of $\{10\bar{1}1\}$ twins, in turn, was explained by the very high yield strength of the concentrated alloy, due to the strong SRO introduced by Gd. The same work, and in line with prior work in Mg-Zn [16], assigned twinning a determining role in the Hall-Petch behavior of alloys. When twinning is activated at small strain, a lower stress intensity factor, k, is expected, whereas when solute interferes with the activation of twinning, twinning is delayed and k increases. The study of the anelastic effect offers a straightforward way to characterise how twinning develops as a function of the applied stress and strain for the given alloy, and this was the driving force for the present study. This is required to understand the role of twinning on the Hall-Petch behavior of Mg alloys and also to correct the 0.2% yield strength data accounting for anelasticity.

In this work, the effect of solute concentration on the anelastic behavior in Mg-Gd alloys was studied, in tension and compression, and for different grain sizes. The presence of SRO has been confirmed by diffuse x-ray scattering in this alloy system

[18], and a behavior akin, only stronger, to that of the Mg-Zn alloys was anticipated. The solute contents were selected to cover the range of dilute (Gd < 0.4 at.%) and concentrated (up to 4.5 at.%) solid solutions.

2. Experimental Procedure

Pure Mg and Mg-Gd alloys with 0.4, 1.5 and 4.2 at % were selected for the present study. Commercial purity magnesium was melted in an electric resistance furnace and predetermined amounts of Mg-40.5 wt.% Gd master alloy were added. Different amounts of Zr in the form of Mg-22.5 wt.% Zr master alloy were added to the melt as a grain refiner to achieve different grain sizes for each alloy composition. The melt was stirred for 10 minutes by hand[1] to ensure the dissolution of the solute elements and pouring into either sand, steel or copper mould was carried out at 710-755° C to get different grain sizes employing different cooling rates. Plates of dimensions 150 x 150 x 32 mm^3 from the sand and copper moulds, and cylinders of diameter 70 mm x height 150 mm from the steel mould castings were obtained.

The castings were sectioned into either 10 x 10 x 95 mm^3 or 20 x 20 x 95 mm^3 bars for making tensile samples or diameter 22 mm x height 45 mm cylinders for making compression samples, and these were solution-treated in argon followed by quenching in water. Solution heat treatment was carried out at 535 °C for 3 and 9 hrs for the 0.4 and 1.5% Gd, respectively, and 540 °C for 12 hrs for the 4.2% Gd. The additional time and temperature was given for the concentrated alloys to ensure the complete

[1] *Mechanical stirring resulted in excessive burning of the melt due to the extreme reactivity of Gd.*

dissolution of the precipitates in to the solid solution. The pure Mg specimens were stress-relieved at 250 °C for 2 hrs and furnace cooled.

The chemical composition of the alloys was determined using the inductively coupled plasma atomic emission spectroscopy and the results are shown in Table 1. Samples for grain size measurement were polished to 1 μm diamond finish followed by alumina polishing and etched using acetic – picric acid mixture [20 ml acetic acid, 3 g picric acid, 20 ml H_2O and 50 ml ethanol]. The mean grain sizes calculated over 800 grains using the linear intercept method are listed in Table 1.

Table 1: Chemical composition and mean grain sizes of the alloys.

Material	Fine grain size			Medium grain size			Coarse grain size		
	grain size (μm)	Actual Gd (at.%)	Zr (at.%)	grain size (μm)	Actual Gd (at.%)	Zr (at.%)	grain size (μm)	Actual Gd (at.%)	Zr (at.%)
Mg	55	-	0.16	170	-	0.20	400	-	0.06
Mg-0.4Gd	48	0.37	0.14	188	0.35	0.02	730	0.35	-
Mg-1.5Gd	35	1.25	0.52	120	1.43	0.13	432	1.32	-
Mg-4.2Gd	53	3.92	0.32	160	3.65	0	300	3.90	0.01

Cylindrical tensile specimens of different gauge diameter, according to the grain size, with a gauge length of 25 mm and cylindrical compression specimens of diameter 20 mm and height 40 mm were machined from the heat treated sections. To ensure true

polycrystalline behavior, the specimen gauge diameter to the grain diameter ratio was always maintained greater than 35 for all the mechanical testing samples, except for the tensile samples of the coarsest grain sizes 432 and 730 μm, which was maintained at 15. Cyclic loading – unloading tests (see Fig. 1) were carried out at crosshead speeds ranging between 0.05 and 0.7 mm/ min, the lower speed was used for the lower strain values of the hysteresis loop testing. A pair of opposing, knife-edge averaging extensometers were used to reduce any error in the recorded strain values caused because of sample misalignment. Tension samples were tested until fracture and compression samples were tested up to 7% strain. Data were stored at a rate of 250 points per second.

3. Observations

Fig. 1. Shows a representative loading-unloading flow curve where the terms used in this work are defined.

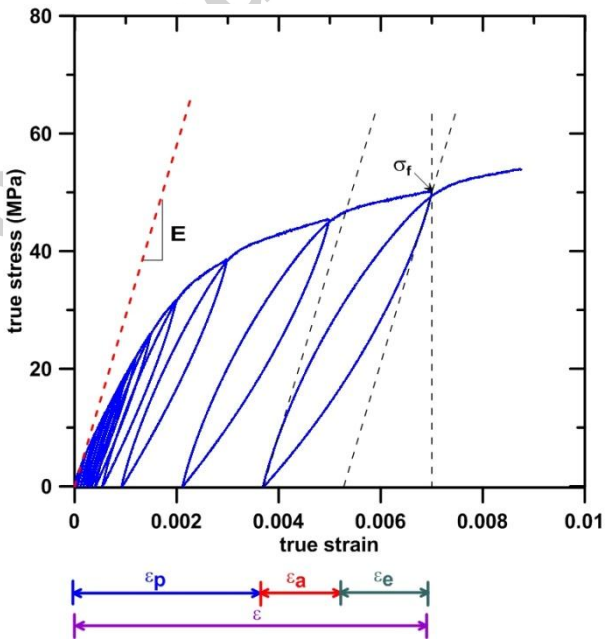

Fig. 1. A tensile loading-unloading test in pure Mg. E is the elastic modulus (44 GPa), σ_f is the flow stress at the start of the unloading; ε_p is the true plastic strain, ε_a the anelastic strain and ε_e the linear elastic strain, at zero load.

Flow curves in tension and compression for the alloys studied are shown in Fig. 2a and b. The strength increased with the Gd content and with the exception of the most concentrated alloy, the loops were wider in compression than in tension. The tensile ductility of the 4.2Gd alloy specimens was very low due to the presence of large oxide films, and that limited the collection of data to strains of about 0.015 [17].

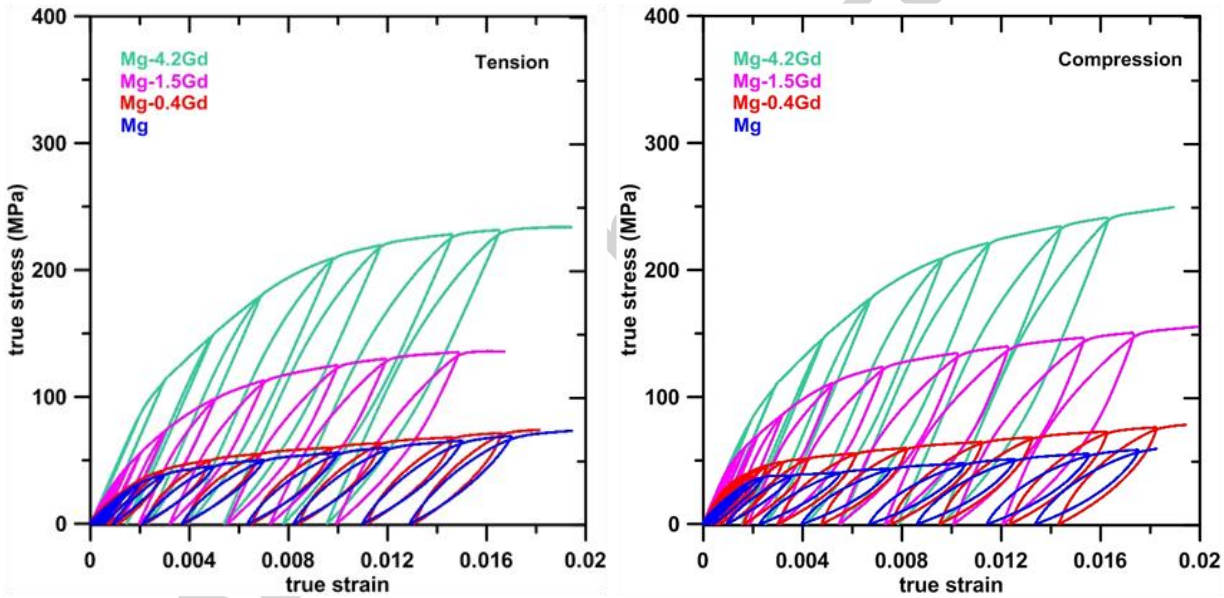

(a) (b)

Fig. 2. Loading-unloading loops: (a) tension, (b) compression. Grain sizes: pure Mg, 170 μm; 0.4Gd, 188 μm; 1.5Gd, 120 μm; 4.2Gd, 160 μm.

The anelastic strain, as defined in Fig. 1, was plotted as a function of true plastic strain for the different alloys and grain sizes in Fig. 3. The anelasticity progressively

developed after an incubation plastic strain, which depended upon the alloy content and grain size; it then reached a maximum at a plastic strain of between 0.01 and 0.025 for all of the alloys and grain sizes.

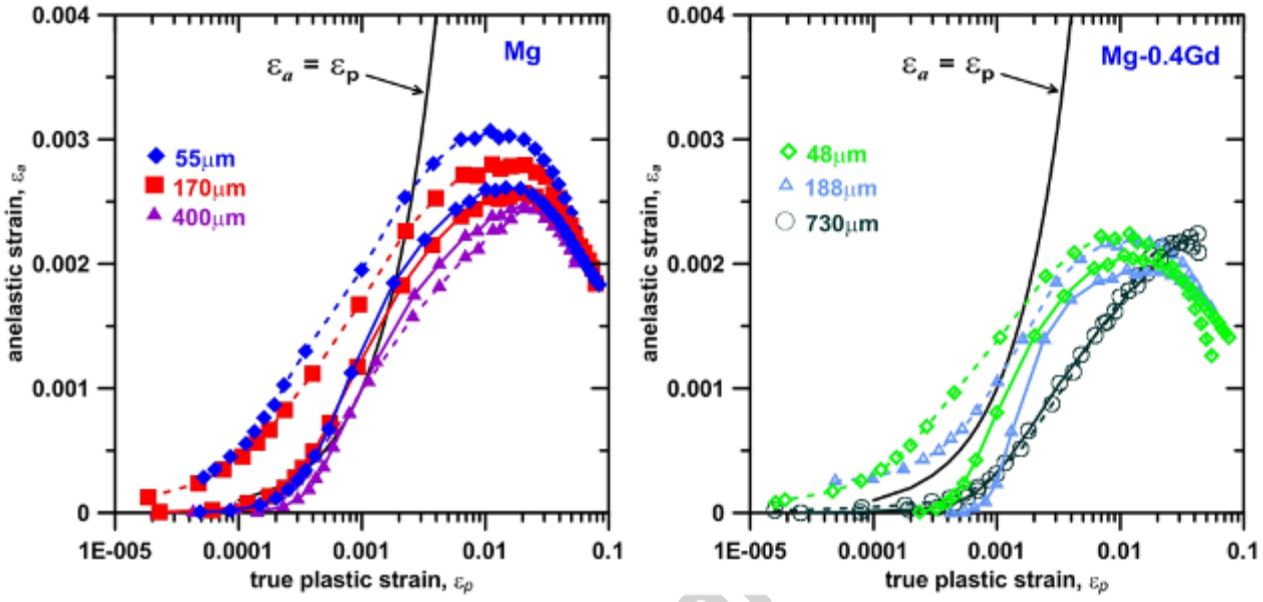

(a)

(b)

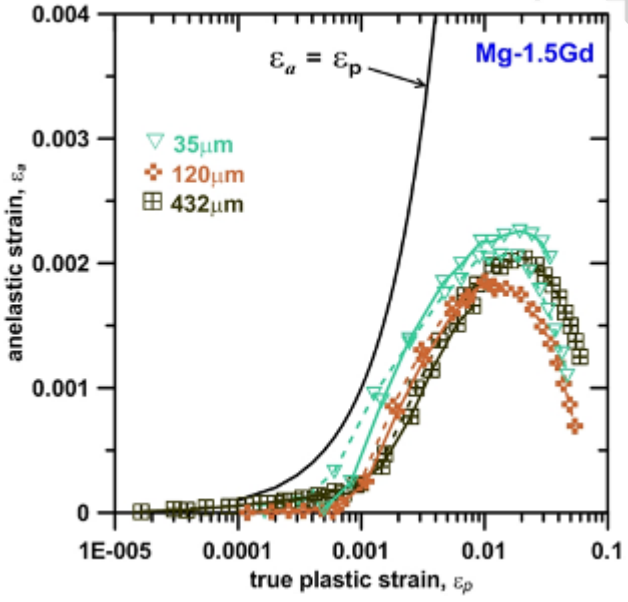

(c)

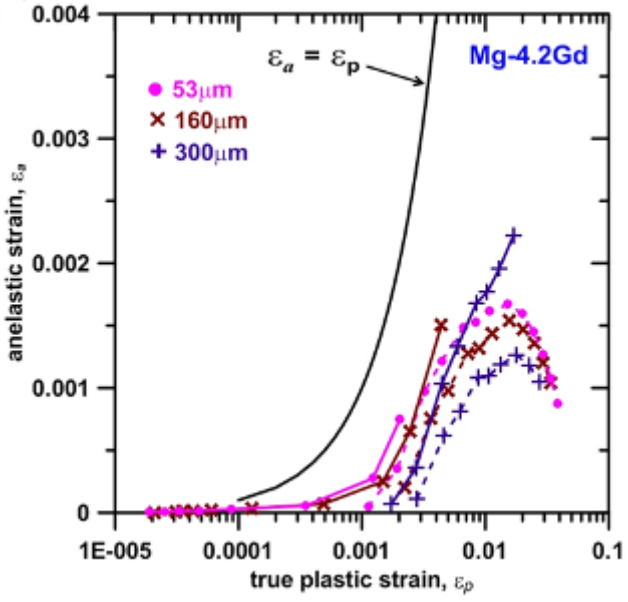

(d)

Fig. 3. The anelastic strain, ε_a, as a function of true plastic strain, ε_p, at different grain sizes of a) pure Mg, b) Mg-0.4% Gd, c) Mg-1.5% Gd, and d) Mg-4.2% Gd alloys, tested in both tension (solid lines) and compression (dashed lines). The line at which $\varepsilon_a = \varepsilon_p$ is drawn for comparison.

Fig. 4 shows that the anelasticity developed at very low plastic strains in pure Mg compared with the alloys. The addition of Gd reduced the magnitude of anelasticity and shifted its onset towards larger strains, keeping it below the $\varepsilon_a = \varepsilon_p$ line for all of the alloys, save for the finer grain size 0.4Gd alloy in compression.

Figs. 5a and b show the effect of grain size and the Gd content, respectively, on the anelastic strain, taken at a plastic strain of 0.002, for the alloys studied. The anelastic strain was generally larger in compression than the tension for all the grain sizes of the pure Mg and Mg-0.4Gd alloy, except for the coarsest grain size where there was no difference between the tension and compression. The anelastic strain was almost same at all the grain sizes for both tension and compression of the 1.5Gd alloy, whereas tension appeared to have more anelastic strain than the compression for the 4.2Gd alloy. Overall the anelastic strain decreased with the increasing grain size for all the materials. The anelastic effect decreased with increasing Gd content and was more pronounced for the finer grains in all materials.

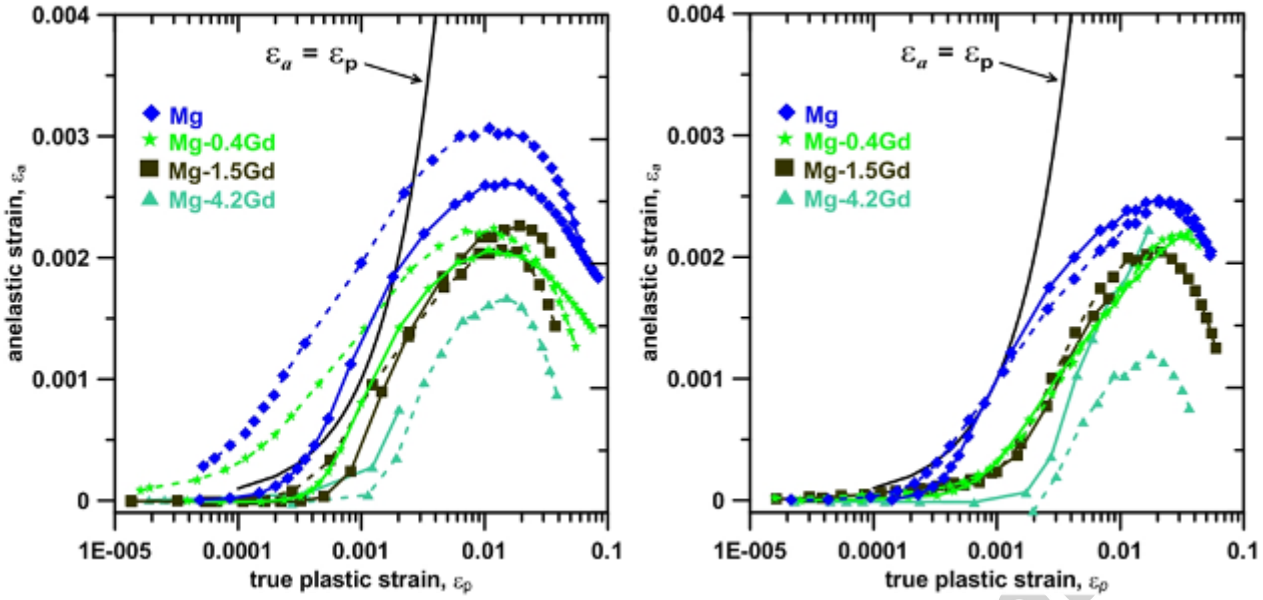

Fig. 4. The anelastic strain, ε_a, as a function of true plastic strain, ε_p, for the alloys studied, in tension (solid lines) and compression (dashed lines). a) Small grain size. (grain sizes: Mg, 55 μm; 0.4Gd, 48 μm; 1.5Gd, 35 μm; 4.2Gd, 53 μm). b) Large grain size. (Mg, 400 μm; 0.4Gd, 730 μm; 1.5Gd, 432 μm; 4.2Gd, 300 μm). The line at which $\varepsilon_a = \varepsilon_p$ is included for reference.

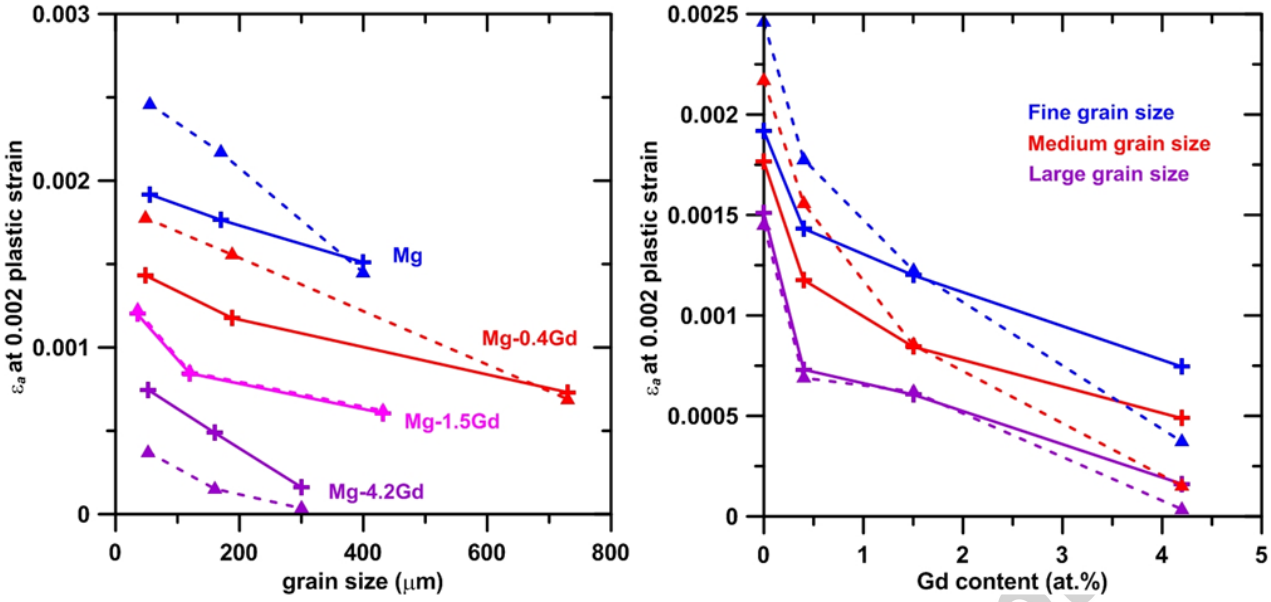

Fig. 5. The anelastic strain, ε_a, as a function of a) grain size, and b) Gd content, for the alloys studied. The crosses and solid lines denote tensile data, the triangles and dashed lines denote compression.

4. Discussion

4.1. Tension-Compression anelastic behavior

The larger anelastic strain in compression than in tension for the pure Mg and the dilute (0.4Gd) alloy is consistent with the notion that the behavior arises from a combination of the polar nature of twinning and the fact that the twin mode with the lowest activation stress is the 'tension" $\{10\bar{1}2\}$ twin: in a random polycrystal, the fraction of grains having their c-axis favourably oriented for (tension) twinning is larger under a compressive stress than under a tensile stress [5, 9-11, 15]. This behavior of the 0.4Gd alloys is consistent with the behavior of the Mg-Zn and Mg-Al alloys reported in [5, 6, 9, 11, 13]. By the same token, the lack of difference between tension and compression for the 1.5Gd alloys, and the reversion, i.e., larger anelastic strain in tension, for the

4.2Gd alloys is puzzling. A possible explanation is put forward when the effects of different solutes is discussed below.

4.2. Grain size effects

The larger anelastic strain at smaller grain sizes is consistent with the idea proposed in [9, 11] that small grain sizes offer more nucleation sites for favourably oriented twinning to occur due to the increased specific grain boundary area. At the same time, smaller twins are less likely to relax plastically, so their tendency to revert can be expected to be larger as well. That is, a reduced grain size is expected to create a larger population of smaller twins, more prone to revert upon unloading, thereby magnifying the anelastic effects.

4.3. Solute concentration

The decrease in the anelastic strain, as well as the shift of the onset to larger strains, with the Gd concentration is consistent with the explanation proposed for Mg-Zn involving SRO [11, 16]. It is known that twinning becomes more difficult when order is present [14], as it makes the atomic shuffling associated with twinning in hexagonal metals more difficult. The total amount of twinning, hence the anelastic strain, is reduced as the strength of the SRO increases.[2] This explanation, however, is at odds with the reversion of the effect at the largest concentration of Gd. To understand why the reversion happens, the effect of other solutes, Al and Zn, must be compared with that of Gd.

[2]*It is noted that* $\{10\bar{1}2\}$ *twins have been recently described as "shuffling dominated" [19-21], a feature that should make this kind of twinning more sensitive to the presence of order than others, such as* $\{10\bar{1}1\}$.

Fig. 6 shows that the addition of solute delays the onset of anelasticity and generally reduces the magnitude of the anelasticity. At the higher end of the solute concentrations, close to the respective terminal solubilities (~2.5 at.% for Zn, ~9 at.% for Al and ~4.2 at.% for Gd), the latter is much more effective in reducing the anelasticity than either Zn or Al, in that order.

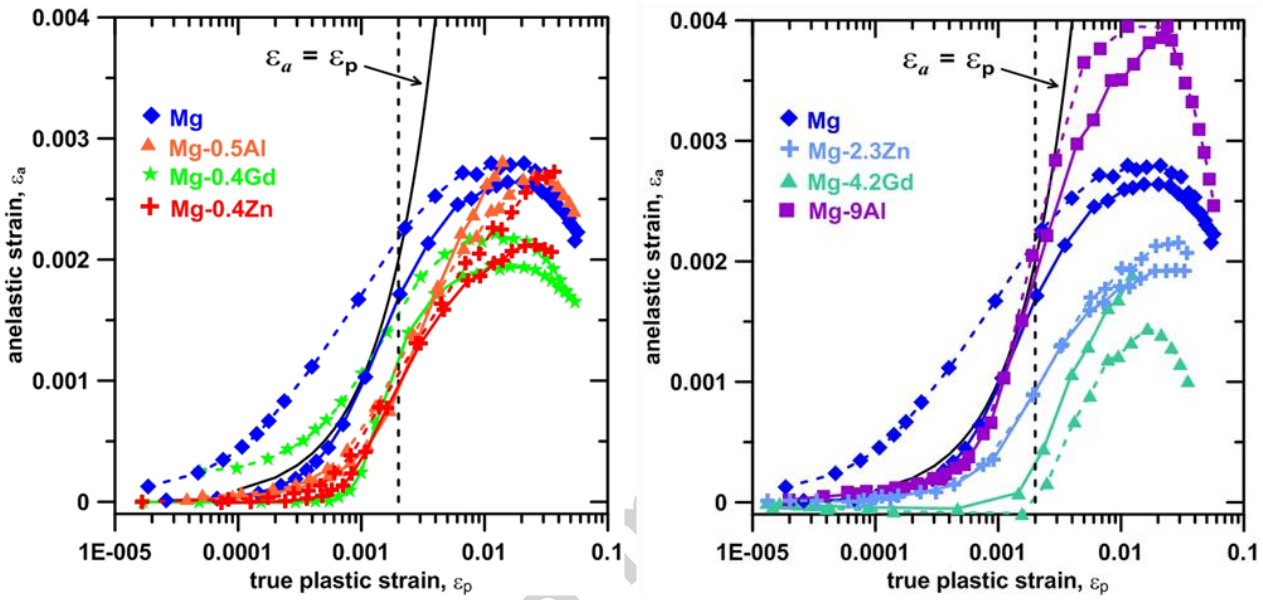

Fig. 6. The anelastic strain, ε_a, as a function of the true plastic strain, ε_p, for different solutes at near constant grain sizes tested in both tension (solid lines) and compression (dashed lines) for a) dilute concentration, b) terminal solid solubility. In a), grain sizes of pure Mg – 170 μm; 0.5Al – 230 μm; 0.4Gd – 188 μm; 0.4Zn – 150 μm. In b), pure Mg – 170 μm; 2.3Zn - 81 μm; 4.2Gd - 160 μm; 9Al – 130 μm. The line at which $\varepsilon_a = \varepsilon_p$ was drawn for comparison. The data for Mg-Al and Mg-Zn alloys are taken from Refs. [10] and [11], respectively.

The stronger (decreasing) effect of Gd concentration on the anelasticity, as well as the reversion (greater anelasticity in tension than in compression) for the 4.2Gd, can be rationalised as follows: The phase diagram indicates that Gd has a stronger tendency[3] to develop short-range order than Zn. The ordering effect of Gd hardens the basal plane as well as increases the CRSS of $\{10\bar{1}2\}$ twinning beyond and above the strengthening introduced by Zn [23]. The higher flow stress of Mg-Gd leads to the activation of $\{10\bar{1}1\}$ twins. The $\{10\bar{1}1\}$ twins differ from the $\{10\bar{1}2\}$ twins in two fundamental aspects: the former are not "shuffling dominated", i.e., they are not expected to be so much affected by the presence of SRO, and they are "compression" type of twins. Thus, they can be expected to make the anelastic effect greater in tension than in compression, therefore accounting for the reversion observed for the 4.2Gd. The increasing trade-off between the hardening of the extension twins and the activation of the compression twins accounts for the increasing reversion of the effect when going from the 0.4Gd to the 4.2Gd. It should be noted that even though the earlier research by Yoo [2] assigned a higher shuffling factor for the $\{10\bar{1}1\}$ twins than for the $\{10\bar{1}2\}$ twins, the reversion of anelastic strain for the 4.2Gd alloy suggests that the $\{10\bar{1}2\}$ twins are more sensitive to the local ordering than the $\{10\bar{1}1\}$ twins.

A third effect must be considered to fully account the effects of the different solutes. The larger difference in CRSS between basal and prism slip in pure Mg enables the activation of $\{10\bar{1}2\}$ twinning at very low stresses and strains, and the large anelasticity in pure Mg follows. The introduction of solute in solution results in solid solution

[3] *The Mg-Gd phase diagram contains 4 different compounds with melting points higher than that of $MgZn_2$, which is consistent with a stronger tendency to developing order in the solid solution in the former [22].*

softening of the prismatic planes, facilitating the activation of prism slip, thereby reducing the participation of twinning as deformation mechanism. Solid solution softening of the prism planes is a general solid solution effect, i.e., it can be expected to operate for all three solutes considered here, Gd, Zn and Al [24]. At higher concentrations, Mg-Zn and Mg-Gd develop SRO, whereas Mg-Al is hardened by much weaker random solid solution effects [25]. The latter has limited effect on the $\{10\bar{1}2\}$ twinning beyond an initial reduction up to about 2 at.% Al. Past that level, it is presumed that solid solution softening is offset by the increased solid solution hardening, and $\{10\bar{1}2\}$ twinning gradually becomes a prominent deformation mechanism again, hence the increased anelasticity at higher concentrations of Al shown by Figure 6-b.

5. Conclusions

The anelastic strain was larger for the pure Mg and decreased with increasing Gd content. The anelasticity was more pronounced for the fine grains in all the materials.

The anelasticity was larger in compression than in tension for the pure Mg and the 0.4Gd alloys. No difference between tension and compression was observed for the 1.5Gd alloys. The anelastic strain in tension was larger than in compression for the 4.2Gd alloys.

The effects can be rationalised by considering the solid solution hardening and softening upon prismatic slip, $\{10\bar{1}2\}$ extension twinning and $\{10\bar{1}1\}$ compression twinning.

Acknowledgements

The author is highly indebted to Prof. Carlos H Caceres and Dr. John R Griffiths for their guidance, support and valuable suggestions on the manuscript. The research work was funded by the Australian Research Council's (ARC) Centre of Excellence for Design in Light Metals program.

References

[1] P.G. Partridge, Metallurgical Reviews, 12 (1967) 169-194.

[2] M.H. Yoo, Metallurgical Transactions, 12A (1981) 409-418.

[3] U.F. Kocks, D.G. Westlake, Transactions AIME, 239 (1967) 1107-1109.

[4] T.W. Duerig, R. Zadno, An engineer's perspective of pseudoelasticity, in: T.W. Duerig (Ed.) Engineering aspects of shape memory alloys, Butterworth-Heineman, Essex, 1990, pp. 369-393.

[5] M.A. Gharghouri, G.C. Weatherly, J.D. Embury, J. Root, Philosophical Magazine, 79 (1999) 1671-1696.

[6] M.A. Gharghouri, McMaster University, Hamilton, Ontario, 1996.

[7] R.L. Woolley, Journal of the Institute of Metals, 83 (1954) 57-58.

[8] E.R.W. Jones, W. Munro, Journal of the Mechanics and Physics of Solids, 1 (1953) 182-188.

[9] C.H. Cáceres, T. Sumitomo, M. Veidt, Acta Materialia, 51 (2003) 6211-6218.

[10] D. Nagarajan, C.H. Caceres, J.R. Griffiths, Acta Physica Polonica A, 122 (2012) 501-504.

[11] G.E. Mann, T. Sumitomo, C.H. Cáceres, J.R. Griffiths, Materials Science and Engineering, 456A (2007) 138-146.

[12] R.E. Reed-Hill, E.P. Dahlberg, W.A. Slippy, Jr., Transactions of the Metallurgical Society of AIME, 233 (1965) 1766-1771.

[13] Z. Keshavarz, M.R. Barnett, in: N.R. Neelameggham, H.I. Kaplan, B.R. Powell (Eds.) Magnesium Technology 2005, TMS (The Minerals, Metals and Materials Society), San Francisco, CA, 2005, pp. 171-175.

[14] J.W. Cahn, Acta Metallurgica, 25 (1977) 1021-1026.

[15] S.R. Agnew, M.H. Yoo, C.N. Tomé, Acta Materialia, 49 (2001) 4277-4289.

[16] C. Caceres, G. Mann, J. Griffiths, Metallurgical and Materials Transactions A, 42 (2011) 1950-1959.

[17] D. Nagarajan, C.H. Caceres, J.R. Griffiths, Metallurgical and Materials Transactions A, 47 (2016) 5401-5408.

[18] D.S. Gencheva, A.A. Katsnel'son, L.L. Rokhlin, V.M. Silonov, F.A. Khavadzha, Fiz. metal. metalloved., 51 (1981) 788-793.

[19] B. Li, H.E. Kadiri, X.Y. Zhang, S.N. Mathaudhu, Q. Ma, Structural Origin of Reversible Twinning, Non-Schmid Effect, Incoherent Twin Boundaries and Texture of Hexagonal Close-Packed Metals, Magnesium Technology 2012, John Wiley & Sons, Inc., 2012, pp. 105-110.

[20] B. Li, E. Ma, Physical Review Letters, 103 (2009) 035503.

[21] A. Kelly, G. W. Groves, P. Kidd, Crystallography and Crystal Defects, Revised Edition ed., John Wiley & Sons, 2000.

[22] P. Haasen, Physical Metallurgy, Cambridge University Press, Cambridge, 1996.

[23] L. Gao, R.S. Chen, E.H. Han, Journal of Alloys and Compounds, 481 (2009) 379-384.

[24] A. Akhtar, E. Teghtsoonian, Acta Metallurgica, 17 (1969) 1351-1356.

[25] C.H. Cáceres, D.M. Rovera, Journal of Light Metals, 1/3 (2001) 151-156.